

1 PRODUCTION OF COPPER LOADED LIPID MICROPARTICLES BY PGSS ®
2 (PARTICLES FROM GAS SATURED SOLUTIONS) PROCESS

3 Víctor Martín¹, Vanessa Gonçalves^{1,2,3}, Soraya Rodríguez-Rojo^{1*}, Daniela Nunes⁴,
4 Elvira Fortunato⁴, Rodrigo Martins⁴, María José Cocero¹, Catarina Duarte^{2,3}

5
6 ¹*High Pressure Processes Group, Department of Chemical Engineering and Environmental Technology, School*
7 *of Engineering. Venue Dr. Mergelina, University of Valladolid. Dr. Mergelina s/n, 47011, Valladolid, Spain*

8 ²*Instituto de Tecnologia Química e Biológica António Xavier, Universidade NOVA de Lisboa, Avenida da Republica,*
9 *2780-157 Oeiras, Portugal*

10 ³*Instituto de Biologia Experimental e Tecnológica, Apartado 12, 2781-901 Oeiras, Portugal*

11 ⁴*i3N/CENIMAT, Department of Materials Science, Faculty of Sciences and Technology, Universidade NOVA de*
12 *Lisboa, Campus de Caparica, 2829-516 Caparica, Portugal*

13 *Corresponding author:

14 E-mail address: sorayarr@iq.uva.es

15

16

17 Abstract

18 Production of lipid particles loaded with metal nanoparticles by supercritical fluids
19 based processes has been barely studied. In this work, copper nanoparticles were loaded
20 into glyceryl palmitostearate microparticles by PGSS® (Particles from Gas Saturated
21 Solutions). The effect of different variables, temperature (60-80 °C), copper load (0.2-
22 5% w/w) and water addition (0 – 40% w/w), in particle size and encapsulation efficiency
23 has been studied. The dispersion of metal nanoparticles in the lipid has been determined
24 by SEM-FIB coupled with EDS mapping. In all cases, mean particle size values lower
25 than 70 µm have been obtained, and encapsulation efficiencies around 60% have been
26 achieved. The addition of water has no negative effect in encapsulation efficiency nor in
27 nanoparticles dispersion within the lipid microparticle, being important since
28 nanoparticles are commonly synthesized in aqueous medium.

29 Keywords: PGSS®; copper nanoparticles encapsulation; lipid microparticles; dispersion

30

31

32 1. Introduction

33 Nanoparticles, especially noble metal nanoparticles, have an emergent importance in
34 biomedicine field. Their uses are diverse, for example, in molecular imaging, targeted
35 drug delivery systems, targeted therapies (hyperthermia, gene silencing or
36 radiotherapy), and biosensors. These wide applications are possible thanks to
37 nanoparticle properties such as specific area, superior narrow range of emission, photo
38 stability, broad excitation wavelength, quantum dots and the possibility of being
39 functionalized [1, 2].

40 One of the most interesting metals is copper. This transition metal has biological
41 activity as anti-inflammatory, anti-proliferative, and biocidal agent, and present some
42 radioisotopes useful for nuclear imaging and radiotherapy [3]. On the other hand,
43 copper organometallic complexes can be used to deliver copper ions or radionuclides to
44 diseased tissues or to modify pharmacokinetics. These copper compounds can be
45 managed by organism since copper is an essential microelement in contrary to other
46 transition metals. For example, copper (II) complexes have anti-inflammatory and anti-
47 proliferative properties and thus could be used in chemotherapy. Moreover, copper in
48 metallic form possesses antimicrobial activity, already used in agriculture. It can
49 degrade DNA by mean of the generation singlet oxygen [4], therefore, it is studied as
50 anti-cancer and anti-proliferative agent [3, 5, 6].

51 In order to apply copper nanoparticles for biomedical applications it is necessary to
52 encapsulate them in order to protect the metal until it arrives to the desired zone, to
53 avoid the damage in healthy cells owing to their cytotoxicity. Since lipids are well
54 tolerated by human body and have low toxicity, they are adequate carriers for the
55 encapsulation of metal nanoparticles. Besides, they present advantages over other

56 colloidal carriers in terms of active compound stability and protection, being possible to
57 be administered in inhalable, transdermal, intravenous or oral form [7].

58 Conventional methods for producing lipid microparticles are microemulsions or double
59 emulsions followed by spray drying or spray chilling [8, 9]. However, these methods
60 involve the use of organic solvents, severe operation conditions and purification steps.

61 PGSS® (Particles from Gas Saturated Solutions) is a technique with the capacity of
62 avoiding conventional technic mentioned drawbacks [10]. In this process, the lipid is
63 melted with the dissolved or suspended active compound, and the final mixture
64 saturated with supercritical carbon dioxide. Then, this suspension is expanded through a
65 nozzle into an expansion chamber and fine copper lipid coated particles are formed [7,
66 11, 12]. One of the advantages of PGSS® in relation to other supercritical fluid
67 technologies is that the substance does not need to be soluble in carbon dioxide, like in
68 the case of Rapid expansion of supercritical solutions (RESS). The production of lipid
69 nanoparticles loaded with metal has been barely studied with this process. Up to the
70 authors knowledge only the group of Bertucco worked on the production of lipid
71 microparticles magnetically active with excellent results using triestearin,
72 phosphatidylcholine and magnetite nanoparticles [13]. In contrast, there are studies
73 about processes in which a polymeric matrix is used in spite of lipid. These processes
74 are based on emulsion technology (microemulsions, miniemulsions, double emulsions)
75 [14, 15]. Further, this process have been combined with supercritical fluid technology
76 for the elimination of the solvent as in the production of, poly (lactic-co-glycolic) acid
77 (PLGA) nanoparticle loaded with magnetite have been formulated by means of
78 supercritical fluid extraction of emulsions [16].

79 In this work, a study of PGSS® process to obtain copper lipid loaded microparticles
80 was performed. The operation conditions were chosen regarding the nature of the lipid

81 used and the variation of its properties when in contact with supercritical carbon dioxide
82 and its influence on the physical properties of the precipitated particles was
83 investigated. Moreover, the effect of metallic nanoparticle load in the product and
84 encapsulation efficiency were studied in order to establish an operational limit. Finally,
85 and since nanoparticles are usually obtained in aqueous dispersion [17], the effect of
86 water in the dispersion of metal in the lipid matrix and particle morphology was
87 observed.

88 2. Materials and methods

89 2.1 Materials

90 Precirol® ATO 5 (glyceryl palmitostearate) was kindly supplied by Gattefossé (France).
91 Imwitor® 600 was supplied by Sasol (Germany). Carbon dioxide with 99.95 mol%
92 purity was delivered by Air Liquide (Portugal). Copper nanoparticles were purchased
93 from Alfa Aesar with a particle size of 20 to 30 nm. All the chemicals have been used
94 without further purification.

95 2.2 Precipitation of copper loaded lipid particles by particles from gas saturated 96 solutions (PGSS®)

97 In order to produce the loaded particles, Precirol 5 ATO is placed in a 50 cm³ high
98 pressure stirred vessel, electrically thermostated at the selected operation temperature.
99 Then, the required amount of copper nanoparticles are added. In the experiments carried
100 out with water, the necessary amount of water and 3 mg of Imwitor® 600 (HLB = 4) are
101 incorporated. Imwitor® is a water/oil emulsifier that is necessary to form a
102 macroemulsion, since Precirol has low hydrophilic lipophilic balance (HLB = 2) [11].
103 In this case, it resulted in an macroemulsion. Thereafter, the vessel is closed and the

104 mixture stirring (150 rpm) begins. Carbon dioxide is pumped by a high pressure
105 pneumatic piston pump to the vessel until experimental pressure is achieved.

106 The mixture and the supercritical carbon dioxide are brought into contact during 15
107 minutes, since no pressure depression was observed after this period being the ideal
108 mixing time [11]. Then, the stirred mixture is depressurized through a nozzle (250 μm)
109 by means of an automated valve to expansion chamber. In this chamber access, the
110 expanded suspension is mixed with compressed air (0.7 MPa, 25°C) for improving
111 drying. The particles are collected in an 18 L container. The equipment flow diagram
112 can be seen in figure 1.

113 (FIGURE 1)

114 Some experiments were performed previously to fix the pressure conditions in the pre-
115 expansion chamber. A value of 10 MPa was selected since an increase in the pressure
116 (up to 15 MPa) did not reduce the particle size, varying also the mixing temperature
117 between the studied range, from 60°C to 80°C. The variables studied apart from
118 temperature were the copper load, from 0.2 to 5%, and the addition of water from 0 to
119 40% of the mass of copper and lipid. Random experiments were repeated showing the
120 good reproducibility of the process.

121 2.3 Particle characterization

122 Particles have been characterized regarding their size distribution, morphology and
123 metal dispersion in the lipid matrix.

124 2.3.1 Particle size distribution of lipid loaded microparticles

125 Particle size distribution was measured by laser diffraction using a Mastersizer 2000
126 (Malvern Instruments) with red light (max. 4 mW helium–neon, 632.8 nm). This

127 equipment has an accuracy and a reproducibility better than 1%. The particles were
128 dispersed in water with surfactant (Pluronic) to improve the dispersion due to the
129 Precirol 5 ATO low HLB. The results are expressed as particle volume distribution
130 average diameter ($d_{0.5}$) and spam. Average diameter and spam values are an average
131 from three different measurements. Spam is defined as the ratio between the $d_{0.5}$ and the
132 difference between $d_{0.9}$ and $d_{0.1}$. If the value is near to 1, the particle size distribution is
133 narrow. Precirol refractive index selected was a generic lipid index (1.6).

134 2.3.2 Morphology and metal dispersion

135 Particle morphology and copper metallic nanoparticles dispersion in the lipid matrix
136 were analyzed by scanning electron microscopy (SEM). Images were taken by a JEOL
137 JSM-820, 20 kV, 23-mm working distance at vacuum conditions equipment. Previous
138 to the analysis, the samples were coated with gold in an argon atmosphere. Furthermore,
139 particles were studied through Focused Ion Beam (FIB) couple to SEM using a Carl
140 Zeiss AURIGA CrossBeam workstation instrument, equipped with an Oxford EDS
141 spectrometer. The particles were dispersed in carbon tape and covered with an Au/Pd
142 conductive film. Ga^+ ions were accelerated to 30 kV at 50 pA. The etching depth is
143 around 0.2 μm .

144 2.4 Chemical characterization

145 The metal load in the particle has been analyzed by inductive coupling plasma with
146 optic emission spectrometry technic (ICP-OES). It was performed with an atomic
147 emission spectrophotometer ICP-OES Varian 725-ES using argon as carrier gas. The
148 samples were digest with nitric acid in a microwave oven in order to oxidize copper to
149 ionic state and eliminate the lipid. The results are expressed as mg of copper per gram

150 of lipid. The method has an error in calibration lower than 2%. Some samples were
151 random repeated in order to check the repeatability of process.

152 Encapsulation efficiency has been calculated from metal load data, as it can be seen in
153 equation 1. C_0 is the theoretical concentration, the product introduced in the process,
154 while C_i is the real concentration measured by ICP.

$$155 \quad \% \text{ encapsulation efficiency} = \frac{C_i}{C_0} \times 100 \quad (1)$$

156 ICP chemical analysis was confirmed by TGA showing similar data in all the cases with
157 a difference between both methods lower than 7%, additionally the amount of water in
158 the final encapsulated product was obtained. The equipment utilized was TGA/SDTA
159 RSI analyzer of Mettler Toledo. Samples of approximately 10 mg were heated from 50
160 °C to 600 °C at a rate of 20 °C/min under N₂ atmosphere (60 N mL/min flow). Water
161 loss was taken into account from 25 °C to 120 °C.

162 3. Results and discussion

163 Before experiments were performed, it was verified that the nanoparticles do not
164 significantly agglomerate when mixing with the carrier material, Precirol, to assure the
165 viability of the process. The mean agglomerate size, as volumetric d_{0.5}, was below
166 100nm, as shown in Figure 1S.

167 Main experimental results are summarized in table 1.

168 (TABLE 1)

169 3.1 Effect of temperature and pressure conditions

170 The selection of range of temperatures used in this work was made in accordance with
171 the lipid melting point variation in the presence of carbon dioxide, studied by A.R.S. de
172 Sousa et al. [18]. The authors verified that the melting point reduces from 63 °C to 50

173 °C, when pressure increases from ambient to 10 MPa, then, the value remains almost
174 constant up to 30 MPa. For this reason, the range of mixing temperature tested has been
175 between 60 °C and 80 °C; the reduction of mixture viscosity improves the atomization
176 of the molten into smaller particles in the depressurization step: increasing the
177 temperature decreases the viscosity of the lipid molten it-self, and lower temperatures
178 increase solubility of carbon dioxide reducing also the viscosity [17][19]. On the other
179 way, it also influences the cooling and solidification rate in the expansion chamber [19],
180 thus smaller particles are expected due to less droplet coalescence if mixing temperature
181 is close to the melting point of the processed material, the lipid in this case.

182 (FIGURE 2)

183 Concerning particle morphology, it is important to observe that the temperature does not
184 have any effect, as it can be seen in figure 2. The same flaked morphology remains
185 when the temperature increased (Images A and B). Similarly, the final particle size does
186 not experiment changes. Figure 3 shows two particle size distributions at different
187 values of temperature, maintaining the other parameters constant. The two distributions
188 are almost identical, meaning that particle formation is almost unaffected by
189 temperature in this experimental conditions due to a counter balance of its influence in
190 the viscosity and cooling rate of the molten, previously discussed.

191 (FIGURE 3)

192 In conclusion, in the studied range conditions, temperature has not effect in the final
193 product morphology and size but it has an obvious effect in the encapsulation. In the
194 experiment 2 at 60 °C, encapsulation efficiency is higher than in experiment 3 at 80 °C.
195 For these reasons, the experiments were performed with the lower values of pressure

196 and temperature (60 °C and 10 MPa), at these conditions, the solubility of carbon
197 dioxide in the lipid is 0.23 g CO₂/g lipid.

198 3.2 Influence of metal dispersion and metal load

199 Microparticles morphology have been analyzed by SEM and SEM-FIB technique. This
200 flaked microparticles (Figure 2) present big hollows irregularly distributed, as shown in
201 the FIB-cut images (Figure 4), and nanoparticles are present in the thin lipid
202 membranes, which define these light structures.

203 The dispersion of copper nanoparticles in the lipid matrix has been measured by EDS
204 mapping of the FIB-cut images (Figure 4).

205 (FIGURE 4)

206 In the experiment with 0.2% of copper without water at 60 °C and 10 MPa (figure 4.a),
207 it can be seen over the particle an homogeneous dispersion of copper because of the red
208 color is in the particle contour uniformly, while in the other three images (4b and 4c),
209 which have 5% of copper, it can be observed tiny particles agglomerations. We can
210 conclude that high copper loading promotes higher degree of nanoparticle
211 agglomeration and hence, worse dispersion of the metal is achieved. Regarding the
212 influence of temperature, comparing figure 4b (60°C) and 4d (80°C) there is no
213 substantial differences between them, although there are not copper agglomerates in the
214 image 4d, as in figure 4a for low copper load due to the lower encapsulation efficiency
215 observed at higher temperature. Also, nanoparticles are slightly better dispersed when
216 the temperature is increased due to the reduction in viscosity in the pre-expansion
217 mixture. Finally, water has not a significant effect in the dispersion, as can be noticed
218 when figures 4b and 4c are compared. This is important since nanoparticles are often

219 produced as aqueous dispersions, and their use as raw material will not affect the
220 process performance with respect to the use of powder nanoparticles.

221 Different values of copper mass were tested. This parameter was varied from 0.007 to
222 0.150 grams, maintaining the total amount in the chamber of 3.000 grams. These values
223 correspond with a theoretical load from 0.2 to 5%. As it can be seen in figure 5, the
224 general trend is that the encapsulation efficiency increases as the mass of copper
225 increases, as expected is there is more copper available to be encapsulated; Besides, the
226 powder agglomeration in the pre-expansion mixture is increased, as previously
227 indicated. It can be noticed that at 0.2% copper load the value of encapsulation
228 efficiency is unusually high; this effect has been observed by other researchers when the
229 amount of material to be encapsulated is very low [20], since it is statistically more
230 probable to be all encapsulated.

231 (FIGURE 5)

232 Regarding particle size, there are not significantly differences associated to mass copper
233 variation (Table 1. experiments 2, 3 and 9) obtaining values between 43 and 49 μm ,
234 unless the experiment with the minimum efficiency, which presents a minor size (33
235 μm).

236 3.3 Initial water influence

237 In numerous processes, it is possible to obtain nanoparticles in aqueous suspension.
238 Thus, trying to reduce separation steps necessities to obtain solid nanoparticles. PGSS®
239 process has been proved with different amounts of water to study the effect in the
240 dispersion and micronization processes.

241 Water content was varied from 0 to 40% to determine its effect in process performance
242 at two different copper loads maintaining the other parameter constant. As previously

243 mentioned, there is no significant effect of water addition in nanoparticles dispersion
244 (Figure 4). Similarly, there is not a significant effect on encapsulation efficiency (figure
245 6) at 5% Cu load, probably due to the fact that the water remains as independent phase
246 and the nanoparticles have affinity by the lipid phase. In table 1 data for experiments
247 carried out at 0.2% copper load is also presented, and in general the same trend is
248 observed, although as commented before due to the small amount present they maybe
249 not fully representative.

250 (FIGURE 6)

251 Similarly, particle size behavior does not present differences regarding water addition to
252 the initial mixture as it can be seen in table 1.

253 (FIGURE 7)

254 Regarding particle morphology, water presence makes flaked particles to be more
255 compact as it can be seen comparing figure 8 with figure 2. Probably due to the longer
256 time required for particle surface solidification that promote the amalgamation of flakes.

257 (FIGURE 8)

258 Finally, through thermogravimetric analysis it is possible to know that the amount of
259 water in the final encapsulate product is below 0.7% for the experiments with the higher
260 amount of water. This is a good result since it indicates that almost all the water is
261 eliminated in expansion process.

262

263 4. Conclusions

264 This work is a preliminary study proving that metal nanoparticles can be successfully
265 incorporated in lipid microparticles by PGSS[®] process. This is a one-step green process
266 that involves the use of carbon dioxide as unique external agent to generate the particles
267 in the micrometric range from a molten mixture.

268 In the tested range of operating conditions ($P = 10$ MPa and $T = 60-80^{\circ}\text{C}$), it has been
269 concluded that the main process parameter is copper content (%). When copper load is
270 augmented the encapsulation efficiency increases without an important influence in
271 particle size, although the metal nanoparticles, which are in general uniformly
272 distributed in the lipid, tends to form small agglomerates.

273 Since metal nanoparticles can be produced as aqueous suspensions, the effect of water
274 addition (up to 40% w/w) has been studied showing no significant effect in
275 encapsulation efficiency nor in nanoparticles dispersion within the lipid microparticle.

276

277

278

279

280 Acknowledgments

281 This work is partially supported by the project Shyman FP7-NMP-2011-LARGE-
282 280983 and the project CTQ2013-44143-R of the Spanish Ministerio de Economía y
283 Competitividad. Víctor Martín thanks the University of Valladolid for his doctoral
284 grant. Soraya Rodríguez-Rojo thanks the Spanish Ministerio de Ciencia e Innovación
285 and the University of Valladolid for her Juan de la Cierva fellowship (JCI-2012-14992).
286 This work was also supported by Fundação para a Ciência e a Tecnologia (FCT)
287 through grant PEst-OE/EQB/LA0004/2011. V. S. S. Gonçalves is also grateful for the
288 financial support from SFRH/BD/77350/2011 grant from FCT. iNOVA4Health -
289 UID/Multi/04462/2013 and UID/Multi/04551/2013 (GreenIT), financially supported by
290 FCT, through national funds and co-funded by FEDER under the PT2020 Partnership
291 Agreement is acknowledged.

292

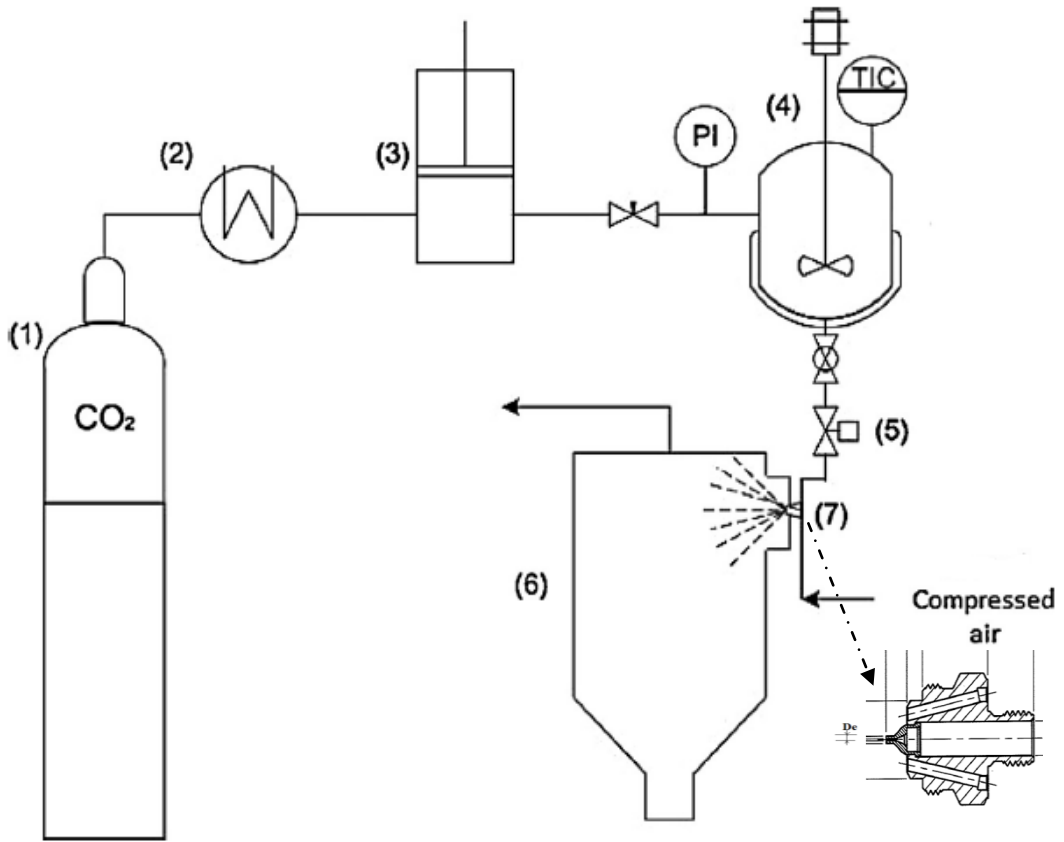
- 294 1. M.S. Amjad, N. Sadiq, H. Qureshi, G. Fareed and S. Sabir, *Nano particles: An emerging*
295 *tool in biomedicine*. Asian Pacific Journal of Tropical Disease, 2015. **5**(10): p. 767-771.
- 296 2. J. Conde, G. Doria and P. Baptista, *Noble metal nanoparticles applications in cancer*. J
297 Drug Deliv, 2012. **2012**: p. 1-12.
- 298 3. P. Szymanski, T. Fraczek, M. Markowicz and E. Mikiciuk-Olasik, *Development of copper*
299 *based drugs, radiopharmaceuticals and medical materials*. Biometals, 2012. **25**(6): p.
300 1089-112.
- 301 4. G.P. Jose, S. Santra, S.K. Mandal and T.K. Sengupta, *Singlet oxygen mediated DNA*
302 *degradation by copper nanoparticles: potential towards cytotoxic effect on cancer*
303 *cells*. J Nanobiotechnology, 2011. **9**: p. 9.
- 304 5. H. Palza, *Antimicrobial polymers with metal nanoparticles*. Int J Mol Sci, 2015. **16**: p.
305 2099-116.
- 306 6. M. Valodkar, R.N. Jadeja, M.C. Thounaojam, R.V. Devkar and S. Thakore, *Biocompatible*
307 *synthesis of peptide capped copper nanoparticles and their biological effect on tumor*
308 *cells*. Materials Chemistry and Physics, 2011. **128**: p. 83-89.
- 309 7. A. R. Sampaio de Sousa, A.L. Simplício, H.C. de Sousa and C.M.M. Duarte, *Preparation*
310 *of glyceryl monostearate-based particles by PGSS®—Application to caffeine*. J. of
311 Supercritical Fluids, 2007. **43**(1): p. 120-125.
- 312 8. A.Puri, K. Loomis, B. Smith, J.H. Lee, A. Yavlovich, E. Heldman and R. Blumenthal, *Lipid-*
313 *Based Nanoparticles as Pharmaceutical Drug Carriers: From Concepts to Clinic*. Crit.
314 Rev. Ther. Drug Carrier Syst., 2009. **26**(6): p. 523-580.
- 315 9. J.H. Kang and Y.T. Ko, *Lipid-coated gold nanocomposites for enhanced cancer therapy*.
316 International Journal of Nanomedicine, 2015. **10**: p. 33-45.
- 317 10. V.S. Goncalves, A.A. Matias, I.D. Nogueira and C.M Duarte, *Supercritical fluid*
318 *precipitation of ketoprofen in novel structured lipid carriers for enhanced mucosal*
319 *delivery--a comparison with solid lipid particles*. Int J Pharm, 2015. **495**(1): p. 302-311.
- 320 11. V.S. Goncalves, S. Rodriguez-Rojo, A.A. Matias, A.V. Nunes, I.D. Nogueira, D. Nunes, E.
321 Fortunato, A.P. de Matos, M.J. Cocero and C.M Duarte, *Development of multicore*
322 *hybrid particles for drug delivery through the precipitation of CO2 saturated emulsions*.
323 Int J Pharm, 2015. **478**(1): p. 9-18.
- 324 12. A. Pestieau, F. Krier, P. Lebrun, A. Brouwers, B. Streel and B. Evrard, *Optimization of a*
325 *PGSS (particles from gas saturated solutions) process for a fenofibrate lipid-based solid*
326 *dispersion formulation*. Int J Pharm, 2015. **485**(1-2): p. 295-305.
- 327 13. K. Vezzù, C. Campolmi and A. Bertucco, *Production of Lipid Microparticles Magnetically*
328 *Active by a Supercritical Fluid-Based Process*. International Journal of Chemical
329 Engineering, 2009. **2009**: p. 1-9.
- 330 14. G.T. Vladislavljevic, *Structured microparticles with tailored properties produced by*
331 *membrane emulsification*. Adv Colloid Interface Sci, 2015. **225**: p. 53-87.
- 332 15. R. Ladj, A. Bitar, M.M. Eissa, H. Fessi, Y. Mugnier, R. Le Dantec and A. Elaissari, *Polymer*
333 *encapsulation of inorganic nanoparticles for biomedical applications*. Int J Pharm,
334 2013. **458**(1): p. 230-41.
- 335 16. M. Furlan, J. Kluge, M. Mazzotti and M. Lattuada, *Preparation of biocompatible*
336 *magnetite-PLGA composite nanoparticles using supercritical fluid extraction of*
337 *emulsions*. J. of Supercritical Fluids, 2010. **54**(3): p. 348-356.
- 338 17. O.V. Kharissova;, H.V. Rasika Dias;, B.I. Kharisov;, B.O. Perez; and V.M. Jimenez Perez;,
339 *The greener synthesis of nanoparticles*. Trends in Biothechnology, 2013. **31**(4): p. 240-
340 248.
- 341 18. A.R.S. de Sousa, M. Calderone, E. Rodier, J. Fages and C.M.M. Duarte, *Solubility of*
342 *carbon dioxide in three lipid-based biocarriers*. J. of Supercritical Fluids, 2006. **39**(1): p.
343 13-19.

- 344 19. P. S. Nalawade, F. Picchioni and L.P.B.M. Janssen, *Supercritical carbon dioxide as a*
345 *green solvent for processing polymer melts: Processing aspects and applications.*
346 *Progress in Polymer Science*, 2006. **31**(1): p. 19-43.
- 347 20. R. Couto, V. Alvarez and F. Temelli (2016) *Encapsulation of Vitamin B2 in solid lipid*
348 *nanoparticles using supercritical CO₂.* *J. of Supercritical Fluids*, DOI:
349 <http://dx.doi.org/10.1016/j.supflu.2016.05.036>.

350

351

352



354

355 Figure 1 Experimental setup FAME Separex: (1) carbon dioxide cylinder, (2) cryostat, (3)
356 pneumatic pump, (4) stirred vessel, (5) depressurization valve, (6) cyclone and (7) nozzle $d=250$
357 μm , with external mixture with compressed air.

358

359

360

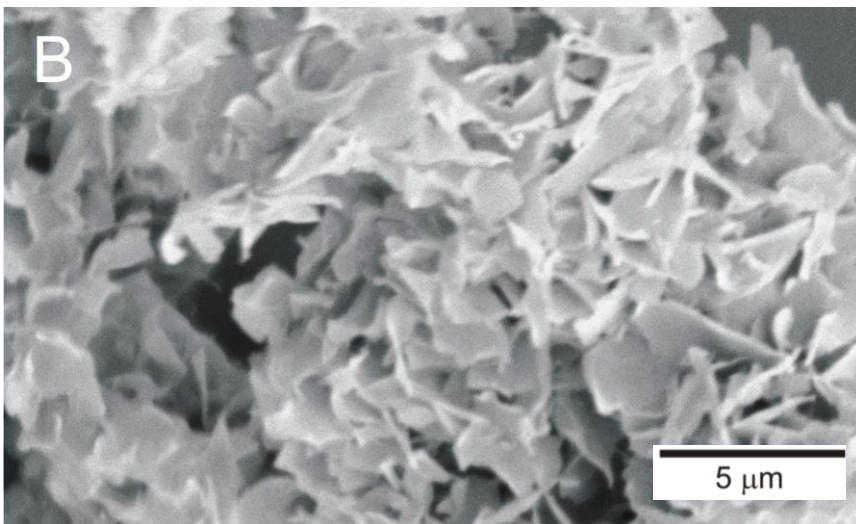
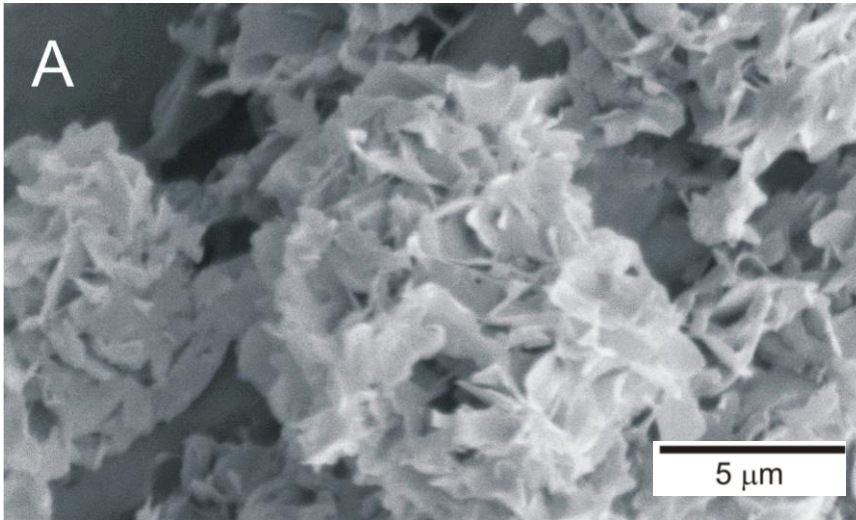
361

362

363

364

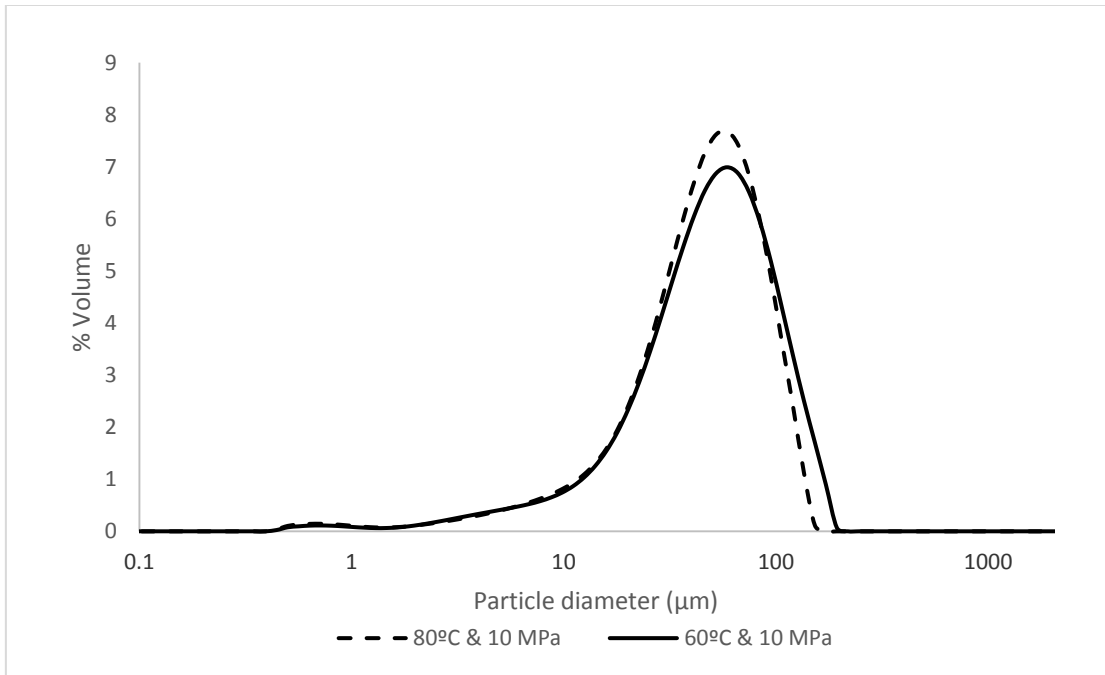
365 Figure 2



368 Figure 2: SEM micrographs of copper-lipid particles produced by PGSS®. Particles in A at 60
369 °C and 10 MPa (Exp. 2, table 1) and particles in picture B at 80 °C and 10 MPa (Exp. 3, table
370 1).

371

372 Figure 3



373

374 Figure 3: Particle size distributions in volume at various temperature conditions (copper load
375 0.2%, water amount near 30%) (Exp. 2 and 3, table 1).

376

377

378

379

380

381

382

383

384

385

386

387

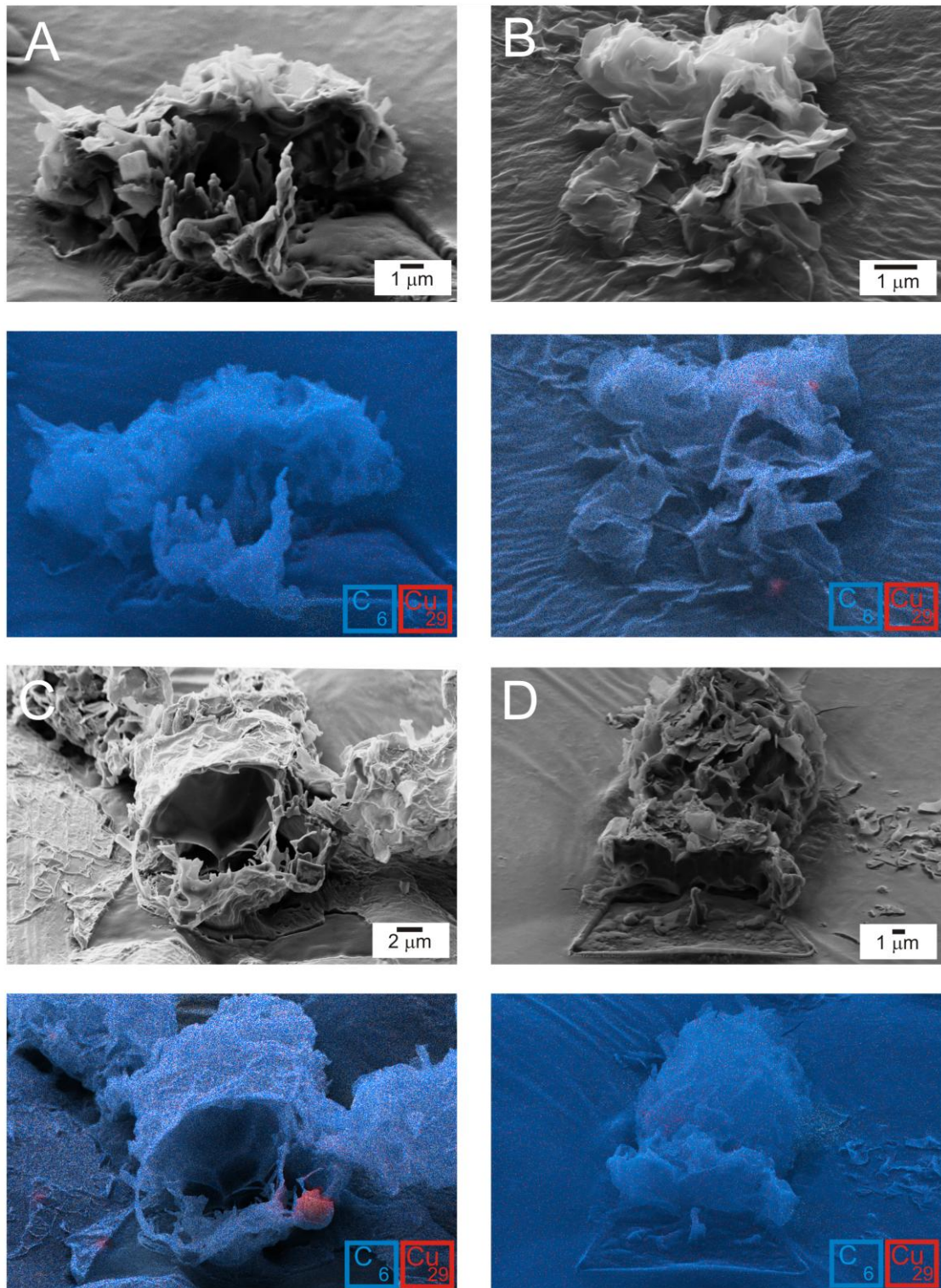
388

389

390

391

392 Figure 4

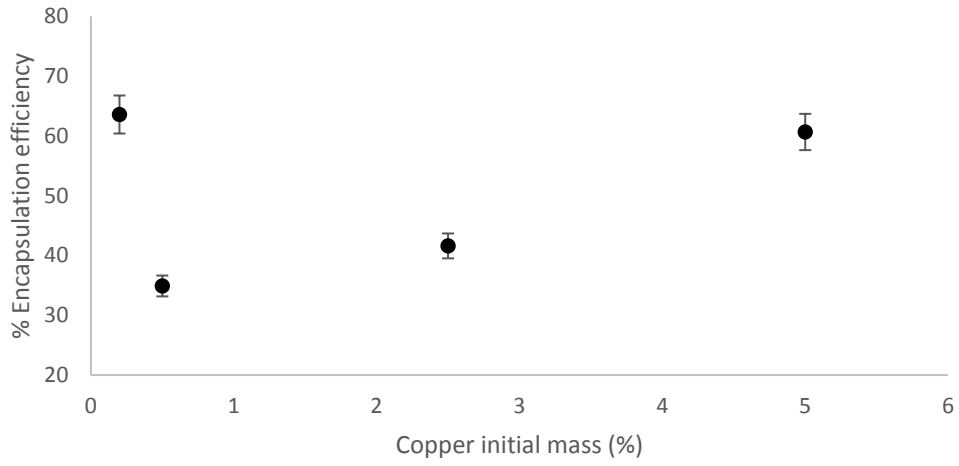


393

394 Figure 4: SEM-FIB analysis of copper loaded lipid particles with EDS mapping (blue-carbon
395 and red-copper): A-0.2% Cu, T = 60 °C , P = 10 MPa, initial water content = 0%, B- 5% Cu,
396 T=60 °C, P= 10 MPa, initial water content = 0%, C- 5% Cu, T=60 °C, P= 10 MPa, initial water
397 content = 40% and D- 5% Cu, T=80 °C, P= 10 MPa, initial water content = 0

398

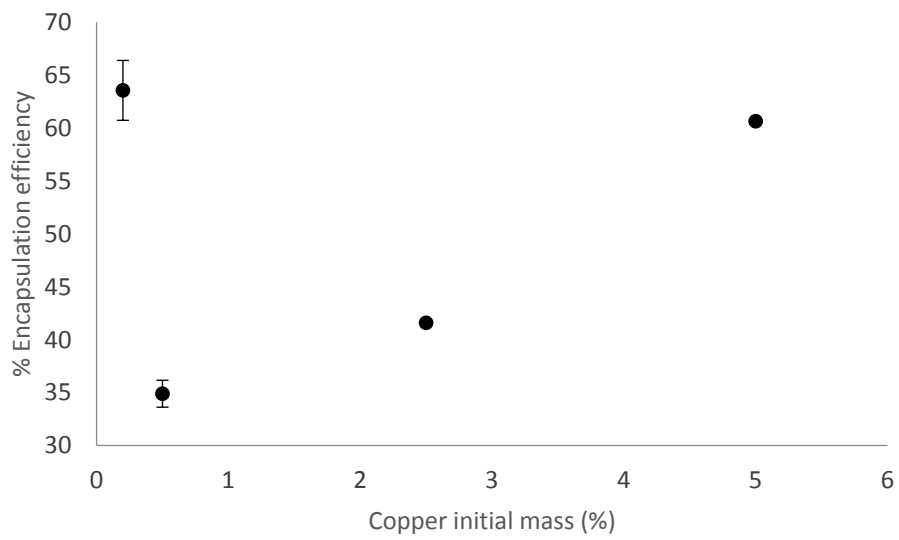
399 Figure 5



400

401

Figure 5: Copper mass influence in encapsulation efficiency.



402

403 Con barras de error de reproducibilidad bien

404

405

406

407

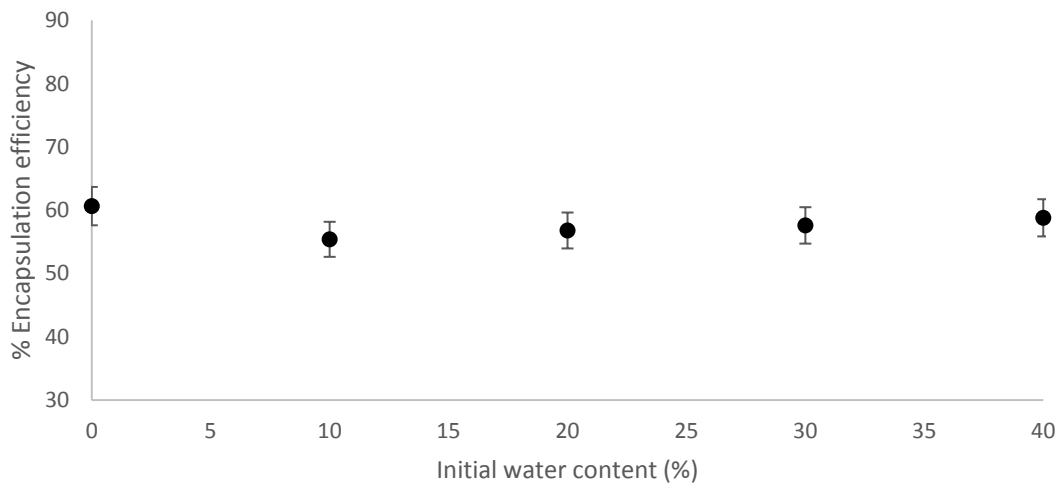
408

409

410

411
412
413
414
415
416
417
418
419
420

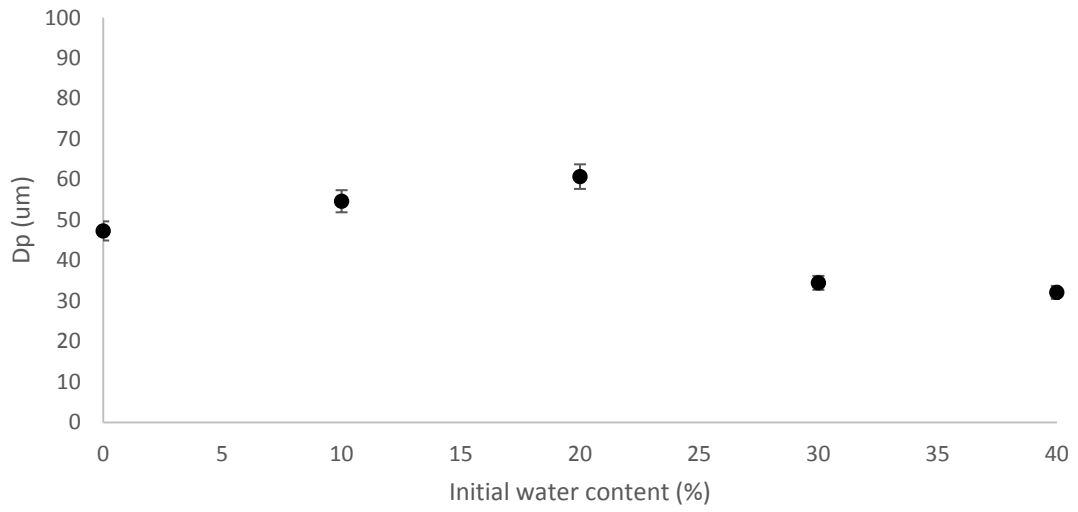
421 Figure 6



422
423
424
425

Figure 6: Variation of encapsulation efficiency with initial content of water (Pressure 10 MPa, temperature 60 °C, 5% Cu load)

426 Figure 7

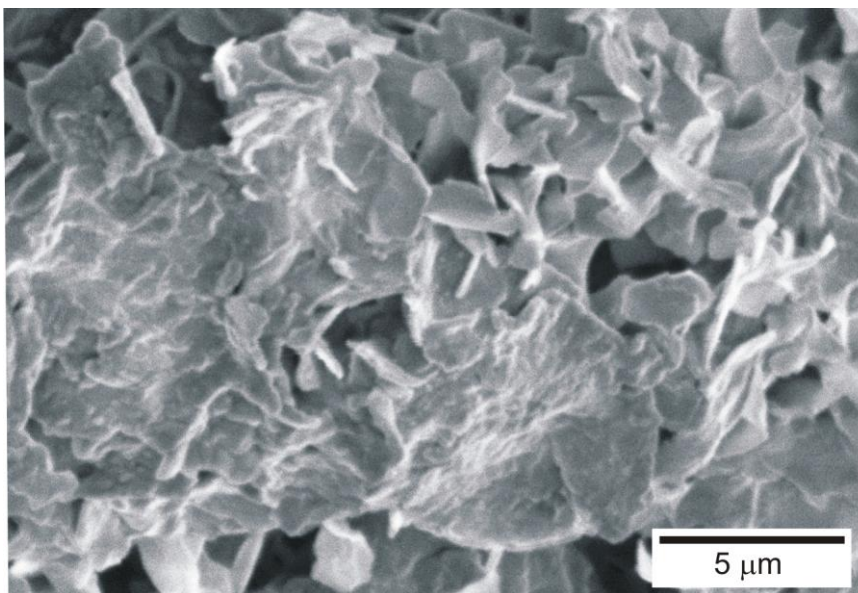


427

428 Figure 7: Variation of final product particle size with initial content of water (Pressure 10 MPa,
429 temperature 60 °C, 5% Cu load)

430

431 Figure 8



432

433 Figure 8: Effect of water in morphology. SEM image from experiment 4 (temperature 60 °C,
434 pressure 10 MPa, copper load 5% and water content 20%).

435 Table 1: PGSS experiment list. En las figuras muestras barras de error para encapsulación y para tamaño
 436 de partícula, aquí deberían aparecer valores con +/-

| Experiment | Precirol (g) | Copper load (w/w%) | Water content* (w/w%) | Temperature (°C) | Encapsulation efficiency (w/w%) | Particle size $d_{0.5}$ (µm) | Particle size spam |
|------------|--------------|--------------------|-----------------------|------------------|---------------------------------|------------------------------|--------------------|
| 1 | 2.985 | 0.5 | 0 | 60 | 35 | 49 | 1.9 |
| 2 | 2.850 | 5.0 | 0 | 60 | 60 | 47 | 1.9 |
| 3 | 2.850 | 5.0 | 0 | 80 | 49 | 45 | 1.7 |
| 4 | 2.850 | 5.0 | 20 | 60 | 57 | 61 | 2.0 |
| 5 | 2.850 | 5.0 | 10 | 60 | 55 | 55 | 1.5 |
| 6 | 2.925 | 2.5 | 0 | 60 | 42 | 33 | 2.0 |
| 7 | 2.850 | 5.0 | 30 | 60 | 58 | 34 | 1.9 |
| 8 | 2.850 | 5.0 | 40 | 60 | 59 | 32 | 1.8 |
| 9 | 2.993 | 0.2 | 0 | 60 | 63 | 41 | 1.6 |
| 10 | 2.993 | 0.2 | 20 | 60 | 64 | 43 | 1.7 |
| 11 | 2.993 | 0.2 | 40 | 60 | 43 | 74 | 1.7 |

437

438 * Water content respect lipid + copper mass.

| Experiment | Precirol (g) | Copper load (w/w%) | Water content* (w/w%) | Temperature (°C) | Encapsulation efficiency (w/w%) | Particle size $d_{0.5}$ (µm) | Particle size spam |
|------------|--------------|--------------------|-----------------------|------------------|---------------------------------|------------------------------|--------------------|
| 1(R) | 2.985 | 0.5 | 0 | 60 | 34.0 ± 1.3 | 49.20±2.83 | 1.9 |
| 2(R) | 2.850 | 5.0 | 0 | 60 | 60.5 ± 0.2 | 47.29±1.20 | 1.9 |
| 3 | 2.850 | 5.0 | 0 | 80 | 49.0 ± 1.0 | 44.59±0.82 | 1.7 |
| 4 | 2.850 | 5.0 | 20 | 60 | 56.8 ± 1.1 | 60.71±2.11 | 2.0 |
| 5 | 2.850 | 5.0 | 10 | 60 | 55.40±1.09 | 54.63±1.92 | 1.5 |
| 6 | 2.925 | 2.5 | 0 | 60 | 41.60±0.83 | 33.42±0.74 | 2.0 |
| 7 | 2.850 | 5.0 | 30 | 60 | 57.60±1.15 | 34.47±0.73 | 1.9 |
| 8 | 2.850 | 5.0 | 40 | 60 | 58.80±1.18 | 32.11±0.68 | 1.8 |
| 9(R) | 2.993 | 0.2 | 0 | 60 | 59.43±2.83 | 41.43±0.20 | 1.6 |
| 10 | 2.993 | 0.2 | 20 | 60 | 63.86±1.28 | 42.73±0.5 | 1.7 |
| 11 | 2.993 | 0.2 | 40 | 60 | 42.86±0.86 | 73.64±3.75 | 1.7 |

439

Supplementary Information

The particle size of the copper nanoparticles dispersed in different media was measured using a dynamic light scattering (DLS) analyzer with a He-Ne laser of 633nm (Zetasizer Nano ZS Malvern Instruments Ltd., Malvern, UK). Dispersions of the necessary amount of copper were prepared using a laboratory magnetic stirrer in water with pluronic F127 as surfactant to improve the wettability of the nanoparticles, and the carriers employed in the PGSS experiments: precirol melted at 60°C and precirol melted with water and imwitor. For each dispersion, about 0.5-1 mL was introduced into the Zetasizer using a disposable cuvette, and particle size was measured 3 times in the DLS equipment and analyzed in duplicate (independent samples). For the samples including precirol the temperature of 60°C was maintained through all the measurement time (ca. 10 min). The volume distribution was used to find out the d0.5 of the particles. Figure 1S shows the results as mean value of the six measurements per sample and standard deviation.

Mean agglomerate size in precirol and precirol + 40% water is 70 +/- 20 nm and 40 +/- 30 nm, respectively, which is significantly lower from the value measured in water with a surfactant (600 +/- 240 nm) were the nanoparticles form big agglomerates and tend to sediment. These results show the affinity of the nanoparticles for the lipid phase.

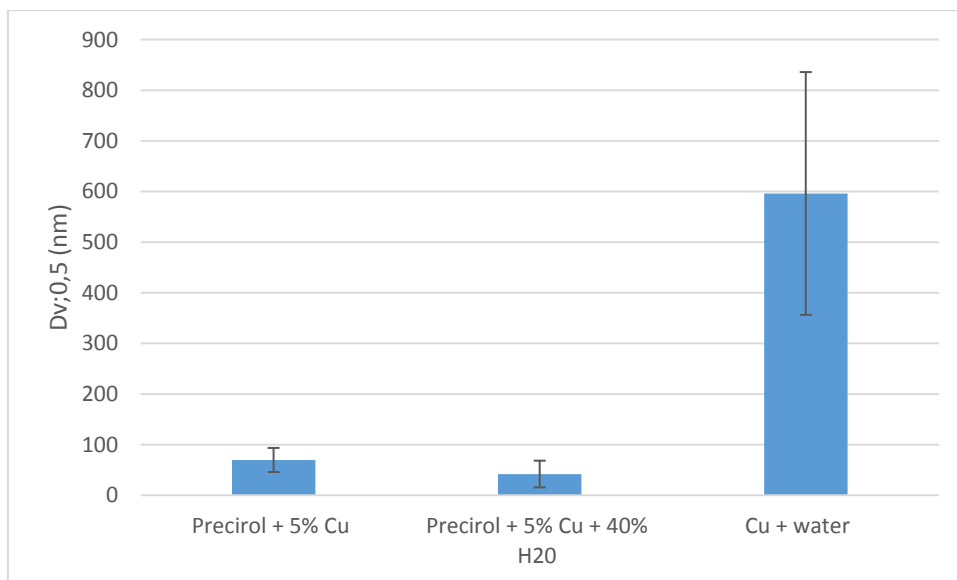


Figure 1S. Nanoparticles agglomerates size (volumetric d0.5) dispersed in different media